Magnetic Field Amplification by Magnetorotational Instability in Core-Collapse Supernovae

Tomasz Rembiasz

Martin Obergaulinger, Pablo Cerdá-Durán, Miguel-Ángel Aloy Torás
Universitat de València

Jérôme Guilet*, Ewald Müller
Max-Planck-Institut für Astrophysik
*Max Planck/Princeton Center for Plasma Physics

CoCoNuT Meeting, Valencia, 14 December 2016

The Supernova Mechanism

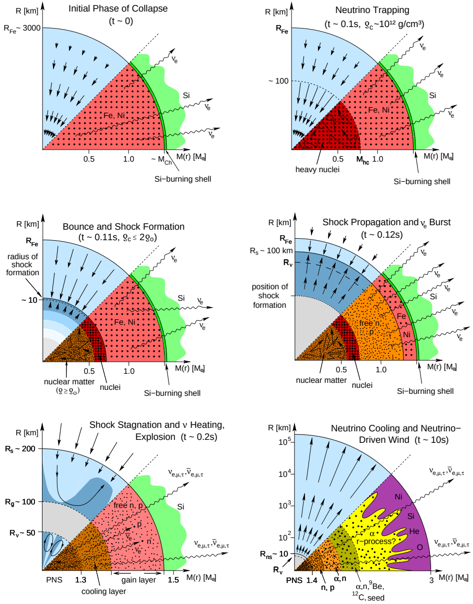

The biggest roles in SN mechanisms are played by

- neutrinos
- standing accretion shock instability (SASI)
- in $< 1\%$ cases MRI (?) (magnetic fields important for $B \gtrsim 10^{15}$ G)

Typical explosion energy $\approx 10^{53} erg$, most of it in neutrinos(!), 'only' $\approx 10^{51} erg$ in kinetic energy.

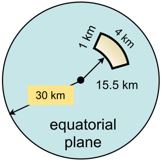

Left panels from Janka et al. (2007)

Magnetic field amplification

- magnetic fields dynamically important for $B \gtrsim 10^{15}$ G
- progenitor's magnetic field $\lesssim 10^9$ G (Heger, Woosley & Spruit 2005)
- core collapse: amplification by compression $10^9\ \mathrm{G} \rightarrow\ 10^{11}\ \mathrm{G}$
- post bounce phase: amplification by convection $10^{11}\ \mathrm{G} \rightarrow 10^{12}\ \mathrm{G}$ (Obergaulinger, Janka & Aloy 2015)
- further amplification by MRI $10^{12}\ \mathrm{G} \rightarrow$?
- amplification by MRI $5 \times 10^{13}\ \mathrm{G} \rightarrow 10^{15}\ \mathrm{G}$ (TR, M. Obergaulinger, P. Cerdá-Durán, E. Müller & M.A. Aloy 2016MNRAS.456.3782R)
- what if you start from realistic magnetic fields?

Resistive-viscous MHD

$$\begin{aligned}
\partial_t \rho + \nabla \cdot (\rho \mathbf{v}) &= 0, \\
\partial_t (\rho \mathbf{v}) + \nabla \cdot (\rho \mathbf{v} \otimes \mathbf{v} + \mathbf{T}) &= -\rho \nabla \Phi, \\
\partial_t e_\star + \nabla \cdot \left[e_\star \mathbf{v} + \mathbf{v} \cdot \mathbf{T} + \eta \left(\mathbf{b} \cdot \nabla \mathbf{b} - \tfrac{1}{2} \nabla \mathbf{b}^2 \right) \right] &= -\rho \mathbf{v} \cdot \nabla \Phi, \\
\partial_t \mathbf{b} - \nabla \times [\mathbf{v} \times \mathbf{b} + \eta (\nabla \times \mathbf{b})] &= 0, \\
\nabla \cdot \mathbf{b} &= 0,
\end{aligned}$$

where $\mathbf{b} \equiv \mathbf{B}/\sqrt{4\pi}$,
$e_\star = \varepsilon + \frac{1}{2}\rho \mathbf{v}^2 + \frac{1}{2}\mathbf{b}^2$; ($\varepsilon$ - internal energy density)
η - resistivity,
Φ - gravitational potential,
$\mathbf{T}$ - stress tensor, i.e.

$$\mathbf{T} = \left[P + \tfrac{1}{2}\mathbf{b}^2 + \rho \left(\tfrac{2}{3}\nu - \xi \right) \nabla \cdot \mathbf{v} \right] \mathbf{I} - \mathbf{b} \otimes \mathbf{b} - \rho \nu \left[\nabla \otimes \mathbf{v} + (\nabla \otimes \mathbf{v})^T \right],$$

ν - kinematic shear viscosity,
ξ - kinematic bulk viscosity.

Our code

- finite-volume Eulerian MHD code AENUS (Obergaulinger 2008)
- HLLD, HLL, LF Riemann solvers (with MUSTA; Toro & Titarev 2006)
- high order reconstruction: monotonicity preserving of 9th, 7th, 5th order (MP9, MP7, MP5; Suresh & Huynh 1997); and piecewise-linear (PL)
- constrained transport to keep $\nabla \cdot \mathbf{B} = 0$ (Evans & Hawley 1998)
- explicit Runge-Kutta time integration (RK2, RK3, RK4)
- resistivity and viscosity can be explicitly added (to the flux terms)

Numerical dissipation ansatz

$$\nu_* = \mathfrak{N}_\nu^{\Delta x} \cdot \mathcal{V} \cdot \mathcal{L} \cdot \left(\frac{\Delta x}{\mathcal{L}}\right)^r + \mathfrak{N}_\nu^{\Delta t} \cdot \mathcal{V} \cdot \mathcal{L} \cdot \left(\frac{\mathcal{V}\Delta t}{\mathcal{L}}\right)^q$$

$\mathcal{V}$ - characteristic velocity,
$\mathcal{L}$ - characteristic length,
r - reconstruction scheme order,
q - time integration scheme order,
$\mathfrak{N}_\nu^{\Delta x}$, $\mathfrak{N}_\nu^{\Delta t}$ - constants

$$\xi_* = \mathfrak{N}_\xi^{\Delta x} \cdot \mathcal{V} \cdot \mathcal{L} \cdot \left(\frac{\Delta x}{\mathcal{L}}\right)^r + \mathfrak{N}_\xi^{\Delta t} \cdot \mathcal{V} \cdot \mathcal{L} \cdot \left(\frac{\mathcal{V}\Delta t}{\mathcal{L}}\right)^q$$

$$\eta_* = \mathfrak{N}_\eta^{\Delta x} \cdot \mathcal{V} \cdot \mathcal{L} \cdot \left(\frac{\Delta x}{\mathcal{L}}\right)^r + \mathfrak{N}_\eta^{\Delta t} \cdot \mathcal{V} \cdot \mathcal{L} \cdot \left(\frac{\mathcal{V}\Delta t}{\mathcal{L}}\right)^q$$

Measuring numerical dissipation

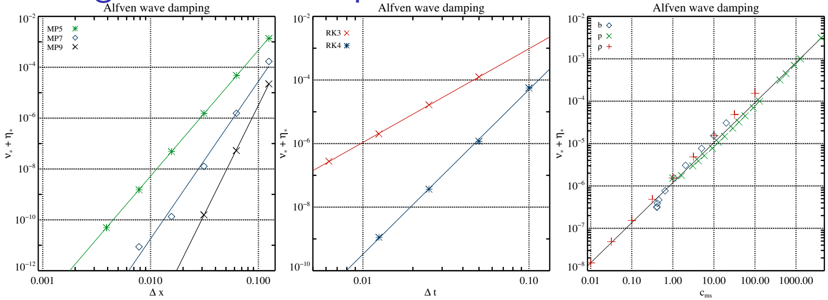

$$\nu_* = \mathfrak{N}_\nu^{\Delta x} \cdot \mathcal{V} \cdot \mathcal{L} \cdot \left(\frac{\Delta x}{\mathcal{L}}\right)^r + \mathfrak{N}_\nu^{\Delta t} \cdot \mathcal{V} \cdot \mathcal{L} \cdot \left(\frac{\mathcal{V}\Delta t}{\mathcal{L}}\right)^q$$

$$\mathcal{V} = c_{\mathrm{ms}}$$

$$\mathcal{L} = \lambda$$

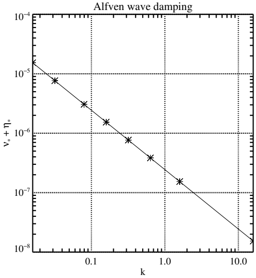

From TR, M. Obergaulinger, P. Cerdá-Durán, M.A. Aloy & E. Müller (2016arXiv161105858R)

Measuring numerical dissipation

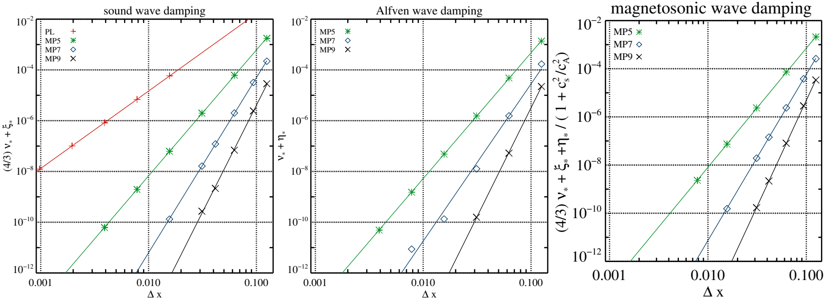

$$\nu_* = \mathfrak{N}_\nu^{\Delta x} \cdot \mathcal{V} \cdot \mathcal{L} \cdot \left(\frac{\Delta x}{\mathcal{L}}\right)^r + \mathfrak{N}_\nu^{\Delta t} \cdot \mathcal{V} \cdot \mathcal{L} \cdot \left(\frac{\mathcal{V}\Delta t}{\mathcal{L}}\right)^q$$

$$\mathcal{V} = c_{\mathrm{ms}}$$

$$\mathcal{L} = \lambda$$

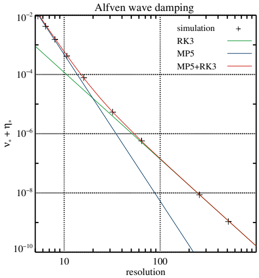

From TR, M. Obergaulinger, P. Cerdá-Durán, M.A. Aloy & E. Müller (2016arXiv161105858R)

Tearing Mode Instability

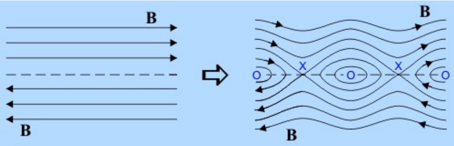

- reconnects magnetic field lines
- its growth-rate

$$\Gamma_{\rm TM} \propto \eta^{4/5} \nu^{-1/5} B^{2/5}$$

(Furth, Killeen & Rosenbluth, 1963)

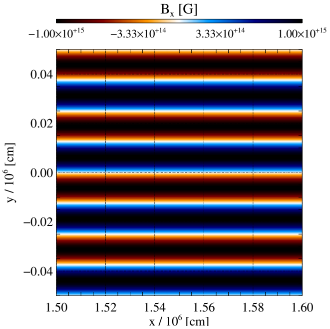

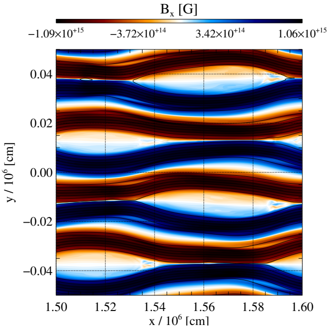

Measuring numerical dissipation

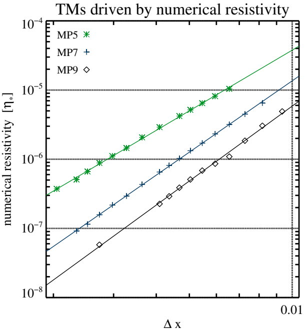

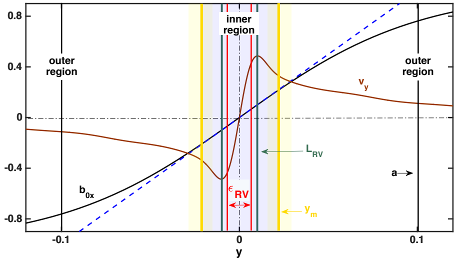

$$\mathcal{V} = c_{\rm ms},$$

but!

$$\mathcal{L} \propto \epsilon_{\rm RV}(\eta, \nu, k, a, c_{\rm A}),$$

and not

$$\mathcal{L} \neq a$$

$$b_{0x}(y) = b_0 \tanh(ay)$$
$$v_{1y} \propto sin(kx)e^{\gamma t}$$

From TR, M. Obergaulinger, P. Cerdá-Durán, M.A. Aloy & E. Müller (2016arXiv161105858R)

Measuring numerical dissipation

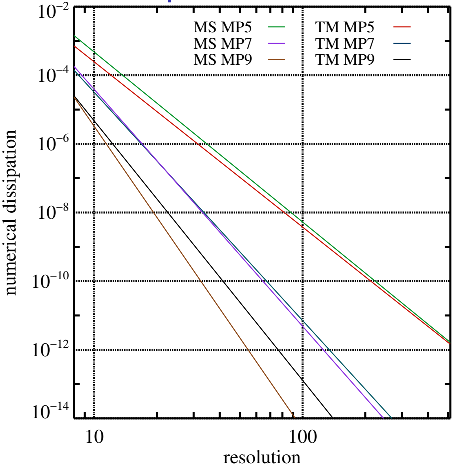

$$\nu_* = \mathfrak{N}_\nu^{\Delta x} \cdot \mathcal{V} \cdot \mathcal{L} \cdot \left(\frac{\Delta x}{\mathcal{L}}\right)^r + \mathfrak{N}_\nu^{\Delta t} \cdot \mathcal{V} \cdot \mathcal{L} \cdot \left(\frac{\mathcal{V}\Delta t}{\mathcal{L}}\right)^q$$

Magnetorotational instability

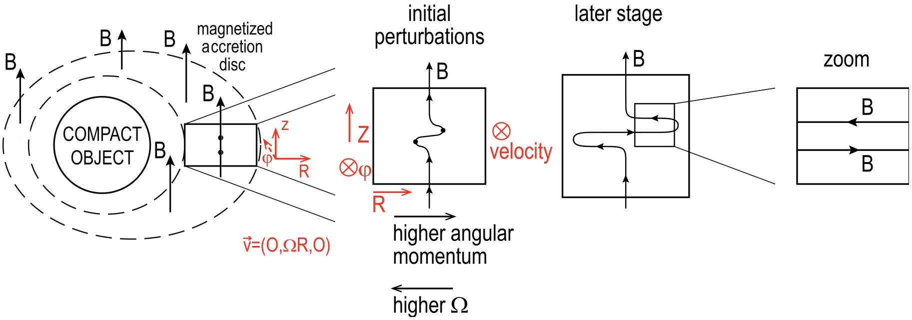

The MRI growth-rate is independent of the initial magnetic field strength

$$\Gamma_{\mathrm{MRI}} = -\frac{\Omega}{2}\frac{\mathrm{d}\ln\Omega}{\mathrm{d}\ln R}$$

$$B_{\mathrm{channel}} \propto V_{\mathrm{channel}} \propto e^{\Gamma_{\mathrm{MRI}} t}$$

Kelvin-Helmholtz Instability

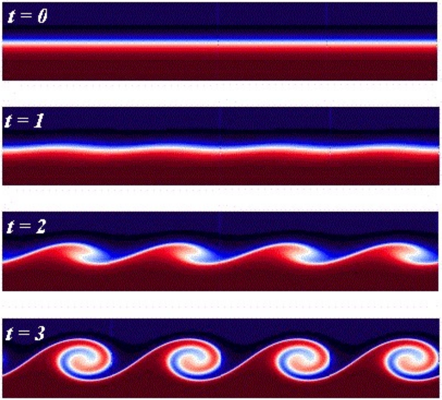

- occurs when there is a velocity shear
- its growth-rate

$$\Gamma_{\mathrm{KH}} \propto V\left(1-\frac{\nu k}{2V}\right),$$

V - velocity,
ν - shear viscosity

MRI and parasitic instabilites

$$B_{\mathrm{channel}} \propto V_{\mathrm{channel}} \propto e^{\Gamma_{\mathrm{MRI}} t}$$

According to Goodman & Xu (1994) and Pessah (2009), on top of MRI channels parasitic instabilities can develop:

- Kelvin-Helmholtz:
  $\Gamma_{\mathrm{KH}} \propto V_{\mathrm{channel}} \propto e^{\Gamma_{\mathrm{MRI}} t}$
- tearing modes:
  $\Gamma_{\mathrm{TM}} \propto \eta^{4/5} B_{\mathrm{channel}}^{2/5} \propto \eta^{4/5} e^{2/5 \times \Gamma_{\mathrm{MRI}} t}$
- when $\Gamma_{\mathrm{KH}} > \Gamma_{\mathrm{MRI}}$ or $\Gamma_{\mathrm{TM}} > \Gamma_{\mathrm{MRI}} \rightarrow$ termination of MRI growth
- MRI amplification:
  $B_z(t=0) \rightarrow B_{\mathrm{channel}}^{\mathrm{term}} = \mathcal{A} B_z(t=0)$,
  where $\mathcal{A}$ is an **amplification factor**

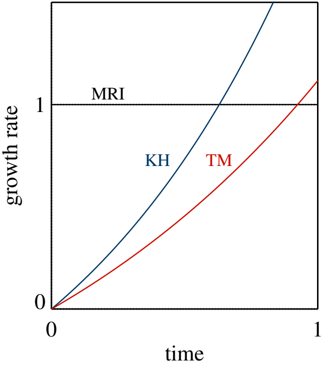

MRI in SNe

- conditions in SNe very different from those in accretion discs
- complex dependence of the turbulent saturated state on the initial conditions (huge parameter space)
- MRI operates on very small length scales ($b = B/\sqrt{4\pi}$):

$$\lambda_{\mathrm{MRI}} \approx 70\ \mathrm{cm} \left(\frac{b}{10^{11}\ \mathrm{G}}\right) \left(\frac{\rho}{2.5 \times 10^{13}\ \mathrm{g\ cm^{-3}}}\right)^{-1/2} \left(\frac{\Omega}{1900\ \mathrm{s^{-1}}}\right)^{-1}$$

- very high-resolution simulations required

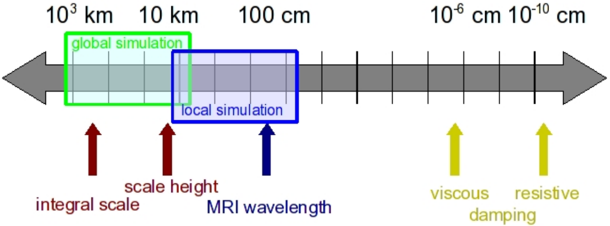

MRI in (numerically) resistive-viscous MHD

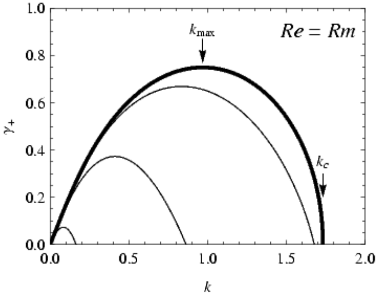

$R_e = R_m = 0.1,\ 1,\ 10,\ \infty$

From Pessah & Chan (2008)

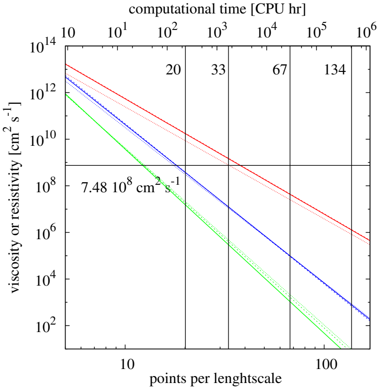

Our goal $R_e^*, R_m^* \leq 100$

From TR, M. Obergaulinger, P. Cerdá-Durán, M.A. Aloy & E. Müller (2016arXiv161105858R)

MRI in (numerically) resistive-viscous MHD

name	reco.	reso.	box	γ_{MRI} [s^{-1}]	$\mathcal{M}_{r\phi}^{\mathrm{term}}$ [10^{30} G^2]
PLM-8	PLM	8	s	926	2.2
PLM-10	PLM	10	s	959	2.3
PLM-16	PLM	16	s	1089	1.9
PLM-20	PLM	20	l	1116	1.9
PLM-34	PLM	34	s	1123	1.8
MP5-8	MP5	8	s	1093	1.1
MP5-10	MP5	10	s	1104	1.4
MP5-16	MP5	16	s	1127	1.05
MP5-20	MP5	20	s	1133	0.82
MP5-34	MP5	34	s	1127	1.03
MP9-8	MP9	8	s	1104	0.79
MP9-10	MP9	10	s	1122	1.3
MP9-16	MP9	16	s	1130	1.1
MP9-20	MP9	20	l	1126	1.1
MP9-25	MP9	25	l	1127	1.0
MP9-34	MP9	34	s	1127	0.93
MP9-67	MP9	67	l	1127	0.73
MP9-134	MP9	134	s	1128	0.73

From TR, M. Obergaulinger, P. Cerdá-Durán,
M.A. Aloy & E. Müller (2016JPhCS.719a2009R)

Simulation box & 3D MRI geometry

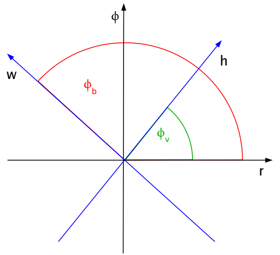

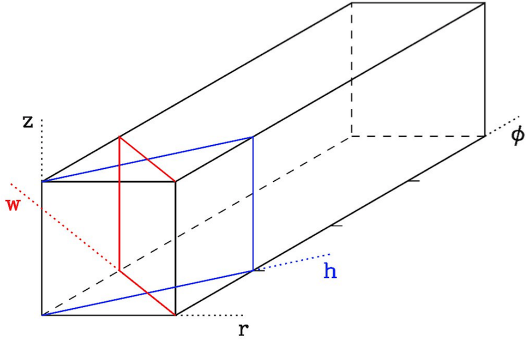

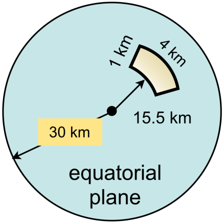

MRI in 3D is terminated by the KH instability

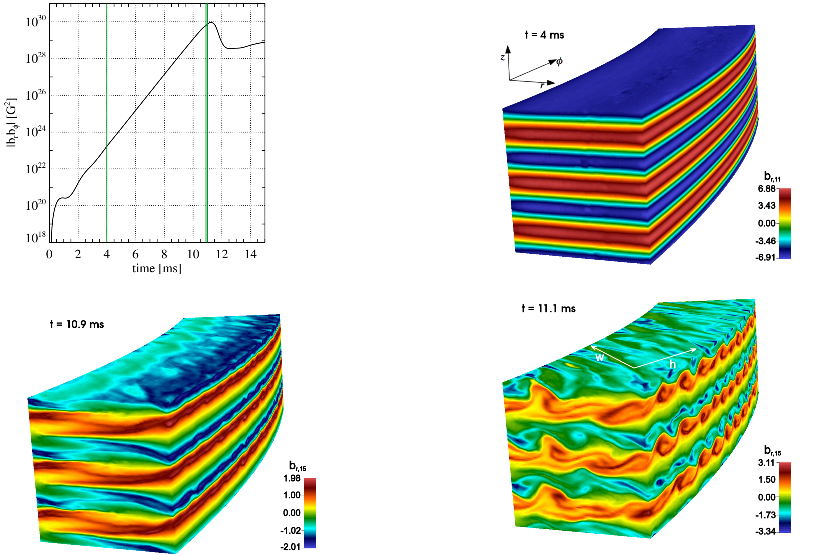

From TR, M. Obergaulinger, P. Cerdá-Durán, E. Müller & M.A. Aloy (2016MNRAS.456.3782R)

MRI in 3D is terminated by the KH instability

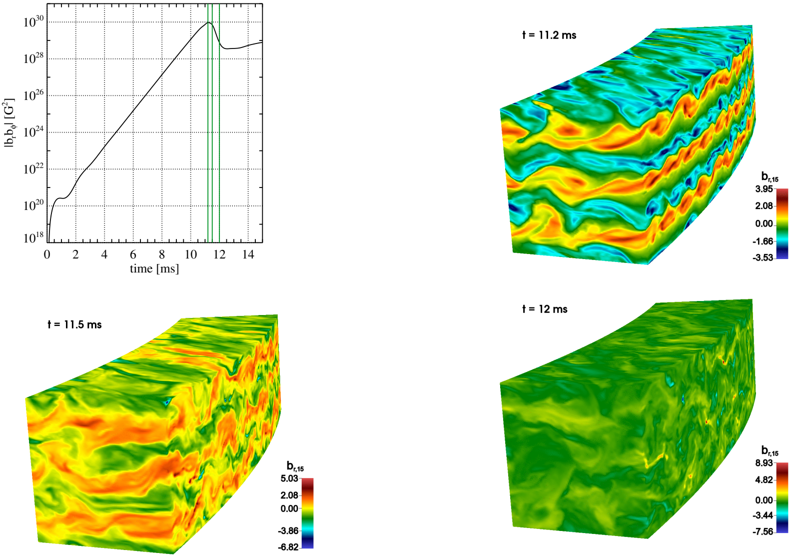

From TR, M. Obergaulinger, P. Cerdá-Durán, E. Müller & M.A. Aloy (2016MNRAS.456.3782R)

MRI termination by the KH insta

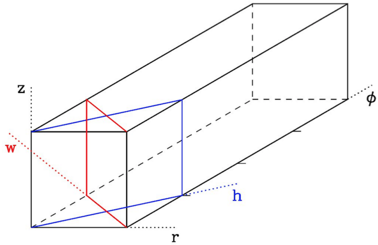

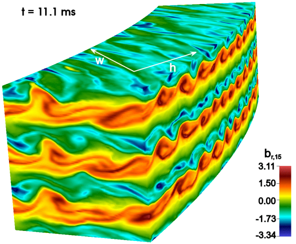

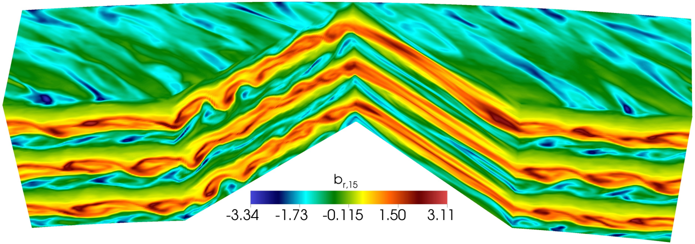

From TR, Obergaulinger, Cerdá-Durán, Müller & Aloy (2016MNRAS.456.3782R)

The MRI termination

For the MP9 reconstruction scheme

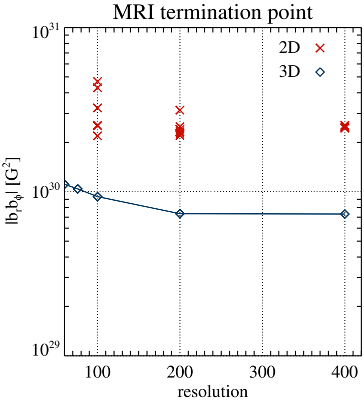

for other reconstruction schemes see
TR, M. Obergaulinger, P. Cerdá-Durán,
M.A. Aloy & E. Müller (2016JPhCS.719a2009R)

- 2D → tearing mode instability

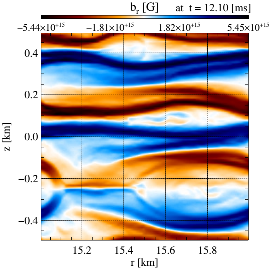

- 3D → Kelvin-Helmholtz instability

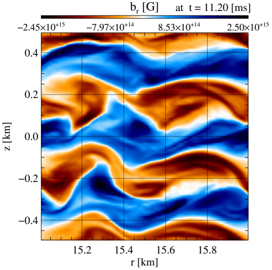

MRI in (numerically) resistive-viscous MHD

name	reco.	reso.	box	γ_{MRI} [s^{-1}]	$\mathcal{M}_{r\phi}^{\text{term}}$ [10^{30} G^2]
PLM-8	PLM	8	s	926	2.2
PLM-10	PLM	10	s	959	2.3
PLM-16	PLM	16	s	1089	1.9
PLM-20	PLM	20	l	1116	1.9
PLM-34	PLM	34	s	1123	1.8
MP5-8	MP5	8	s	1093	1.1
MP5-10	MP5	10	s	1104	1.4
MP5-16	MP5	16	s	1127	1.05
MP5-20	MP5	20	s	1133	0.82
MP5-34	MP5	34	s	1127	1.03
MP9-8	MP9	8	s	1104	0.79
MP9-10	MP9	10	s	1122	1.3
MP9-16	MP9	16	s	1130	1.1
MP9-20	MP9	20	l	1126	1.1
MP9-25	MP9	25	l	1127	1.0
MP9-34	MP9	34	s	1127	0.93
MP9-67	MP9	67	l	1127	0.73
MP9-134	MP9	134	s	1128	0.73

From TR, M. Obergaulinger, P. Cerdá-Durán,
M.A. Aloy & E. Müller (2016JPhCS.719a2009R)

Tracing the parasites (AENUS)

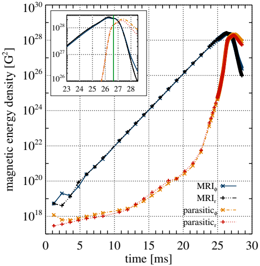

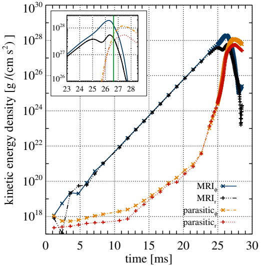

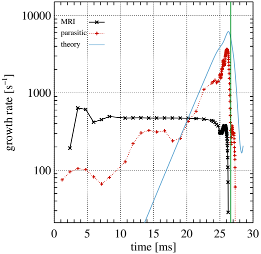

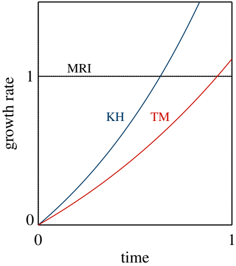

From TR, J. Guilet, M. Obergaulinger, P. Cerdá-Durán, M.A. Aloy & E. Müller (2016MNRAS.460.3316R)

Tracing the parasites (Snoopy)

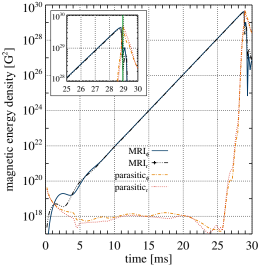

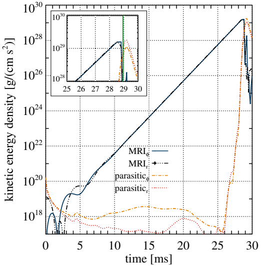

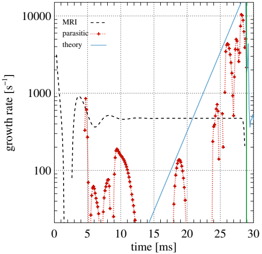

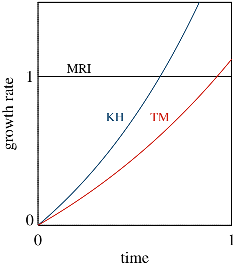

From TR, J. Guilet, M. Obergaulinger, P. Cerdá-Durán, M.A. Aloy & E. Müller (2016MNRAS.460.3316R)

Amplification Factor

- initial magnetic field
- parasitic amplitude
- channel amplitude

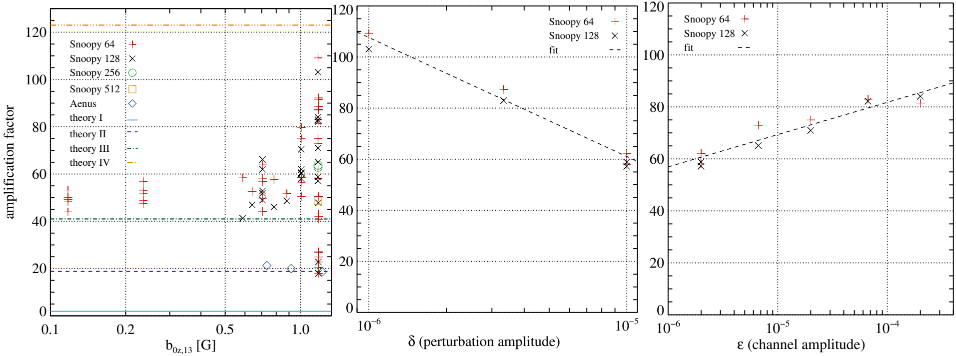

From TR, J. Guilet, M. Obergaulinger, P. Cerdá-Durán, M.A. Aloy & E. Müller (2016MNRAS.460.3316R)

For typical core-collapse SNe, we expect $\mathcal{A} \approx 10$

Conclusions

- 3D simulations indicate that the MRI grows by a factor of $\mathcal{A} \approx 20$, therefore
- magnetic field amplification from 10^{12} G to 10^{15} G is hard to achieve by MRI channel modes
- further amplification by (?): MRI-driven turbulence, large-scale dynamo, ...

Thank you for your attention!